4.01
Ozone, Hydroxyl Radical, and Oxidative Capacity

R. G. Prinn

Massachusetts Institute of Technology, Cambridge, MA, USA

4.01.1 INTRODUCTION 1
4.01.2 EVOLUTION OF OXIDIZING CAPABILITY 3
4.01.2.1 Prebiotic Atmosphere 4
4.01.2.2 Pre-industrial Atmosphere 5
4.01.3 FUNDAMENTAL REACTIONS 5
4.01.3.1 Troposphere 5
4.01.3.2 Stratosphere 7
4.01.4 METEOROLOGICAL INFLUENCES 8
4.01.5 HUMAN INFLUENCES 9
4.01.5.1 Industrial Revolution 9
4.01.5.2 Future Projections 10
4.01.6 MEASURING OXIDATION RATES 11
4.01.6.1 Direct Measurement 11
4.01.6.2 Indirect Measurement 13
4.01.7 ATMOSPHERIC MODELS AND OBSERVATIONS 16
4.01.8 CONCLUSIONS 16
REFERENCES 17

4.01.1 INTRODUCTION

The atmosphere is a chemically complex and dynamic system interacting in significant ways with the oceans, land, and living organisms. A key process proceeding in the atmosphere is oxidation of a wide variety of relatively reduced chemical compounds produced largely by the biosphere. These compounds include hydrocarbons (RH), carbon monoxide (CO), sulfur dioxide (SO_2), nitrogen oxides (NO_x), and ammonia (NH_3) among others. They also include gases associated with advanced technologies such as hydrofluoro carbons and hydrochlorofluorocarbons. A summary of the composition of the atmosphere at the start of the twenty-first century is given in Table 1. Due to their key role, oxidation reactions are sometimes referred to as nature's atmospheric "cleansing" process, and the overall rate of this process as the "oxidation capacity" of the atmosphere. Without this efficient cleansing process, the levels of many emitted gases could rise so high that they would radically change the chemical nature of our atmosphere and biosphere and, through the greenhouse effect, our climate.

Oxidation became an important atmospheric reaction on Earth once molecular oxygen (O_2) from photosynthesis had reached sufficiently high levels. This O_2 could then photodissociate in the atmosphere to give oxygen atoms, which combine with O_2 to form ozone (O_3). When O_3 absorbs UV light at wavelengths less than 310 nm, it produces excited oxygen atoms ($O(^1D)$) which can attack water vapor to produce the hydroxyl free radical (OH). It is the hydroxyl radical that, above all, defines the oxidative capacity of our O_2- and

Table 1 Gaseous chemical composition of the atmosphere (1 ppt = 10^{-12}, 1 ppb = 10^{-9}, 1 ppm = 10^{-6}).

Constituent	*Chemical formula*	*Mole fraction in dry air*	*Major sources*
Nitrogen	N_2	78.084%	Biological
Oxygen	O_2	20.948%	Biological
Argon	Ar	0.934%	Inert
Carbon dioxide	CO_2	360 ppm	Combustion, ocean, biosphere
Neon	Ne	18.18 ppm	Inert
Helium	He	5.24 ppm	Inert
Methane	CH_4	1.7 ppm	Biogenic, anthropogenic
Hydrogen	H_2	0.55 ppm	Biogenic, anthropogenic, photochemical
Nitrous oxide	N_2O	0.31 ppm	Biogenic, anthropogenic
Carbon monoxide	CO	50–200 ppb	Photochemical, anthropogenic
Ozone (troposphere)	O_3	10–500 ppb	Photochemical
Ozone (stratosphere)	O_3	0.5–10 ppm	Photochemical
NMHC	C_xH_y	5–20 ppb	Biogenic, anthropogenic
Chlorofluorocarbon 12	CF_2Cl_2	540 ppt	Anthropogenic
Chlorofluorocarbon 11	$CFCl_3$	265 ppt	Anthropogenic
Methylchloroform	CH_3CCl_3	65 ppt	Anthropogenic
Carbon tetrachloride	CCl_4	98 ppt	Anthropogenic
Nitrogen oxides	NO_x	10 ppt–1 ppm	Soils, lightning, anthropogenic
Ammonia	NH_3	10 ppt–1 ppb	Biogenic
Hydroxyl radical	OH	0.05 ppt	Photochemical
Hydroperoxyl radical	HO_2	2 ppt	Photochemical
Hydrogen peroxide	H_2O_2	0.1–10 ppb	Photochemical
Formaldehyde	CH_2O	0.1–1 ppb	Photochemical
Sulfur dioxide	SO_2	10 ppt–1 ppb	Photochemical, volcanic, anthropogenic
Dimethyl sulfide	CH_3SCH_3	10–100 ppt	Biogenic
Carbon disulfide	CS_2	1–300 ppt	Biogenic, anthropogenic
Carbonyl sulfide	OCS	500 ppt	Biogenic, volcanic, anthropogenic
Hydrogen sulfide	H_2S	5–500 ppt	Biogenic, volcanic

Source: Brasseur *et al.* (1999) and Prinn *et al.* (2000).

H_2O-rich atmosphere (Levy, 1971; Chameides and Walker, 1973; Ehhalt, 1999; Lelieveld *et al.*, 1999; Prather *et al.*, 2001). As of early 2000s, its global average concentration is only $\sim 10^6$ radicals cm^{-3} or ~ 6 parts in 10^{14} by mole in the troposphere (Prinn *et al.*, 2001). But its influence is enormous and its life cycle complex. For example, it reacts with CO, usually within ~ 1 s, to produce CO_2 (and also a hydrogen atom, which quickly combines with O_2 to form hydroperoxy free radicals, HO_2). Another key player is nitric oxide (NO), which can be produced by lightning, combustion, and nitrogen microbes, and undoubtedly became present at significant levels in the Earth's atmosphere as soon as O_2 and N_2 became the dominant atmospheric constituents. NO can react with either O_3 or HO_2 to form NO_2. The reaction of NO with HO_2 is special because it regenerates OH giving two major sources ($O(^1D) + H_2O \rightarrow 2OH$ and $NO + HO_2 \rightarrow NO_2 + OH$) for this key cleansing radical. The NO_2 is also important because it photodissociates even in violet wavelengths to produce oxygen atoms and thus O_3. Hence, there are also two major sources of O_3 (photodissociation of both O_2 and NO_2).

Table 2 Global turnover of tropospheric trace gases and the fraction removed by reaction with OH according to Ehhalt (1999). The mean global OH concentration was taken as 1×10^6 cm^{-3} (Prinn *et al.*, 1995) (1 Tg = 10^{12}g).

Trace gas	*Global emission rate* (Tg yr^{-1})	*Removal by OH* (%)	*Removal by OH* (Tg yr^{-1})
CO	2,800	85	2,380
CH_4	530	90	477
C_2H_6	20	90	18
Isoprene	570	90	513
Terpenes	140	50	70
NO_2	150	50	75
SO_2	300	30	90
$(CH_3)_2S$	30	90	27

The importance of OH as a removal mechanism for atmospheric trace gases is illustrated in Table 2, which shows the global emissions of each gas and the approximate percentage of each of these emitted gases which is destroyed by reaction with OH (Ehhalt, 1999).

Evidently, OH removes a total of $\sim 3.65 \times 10^{15}$ g of the listed gases each year, or an

amount equal to the total mass of the atmosphere every 1.4×10^6 yr. Without OH our atmosphere would have a very different composition, as it would be dominated by those gases which are presently trace gases.

Because both UV radiation fluxes and water vapor concentrations are largest in the tropics and in the southern hemisphere, the levels of OH generally have their maxima in the lower troposphere in these regions and seasons (Figure 1). Also, because much O_3 is produced in and exported from polluted areas, its concentrations generally have maxima in the northern hemisphere mid-latitude summer (Figure 1).

Even from the very brief discussion above, it is clear that the levels of OH in the atmosphere are not expected to remain steady but to change rapidly on a wide variety of space and timescales. In the lower atmosphere, OH sources can be decreased or turned off by lowering UV radiation (night time, winter, increasing cloudiness, thickening stratospheric O_3 layer), lowering NO emissions, and lowering H_2O (e.g., in a cooling climate). Its sinks can be increased by increasing emissions of reduced gases (CO, RH, SO_2, etc.). Hence, OH levels are expected to have changed substantially over geological and even recent times. But because natural or anthropogenic combustion of biomass or fossil fuel is a primary source of gases driving the oxidation processes, and because CO and NO are both products of combustion with (usually) opposite effects on OH levels, the system is not as unstable as it could otherwise be.

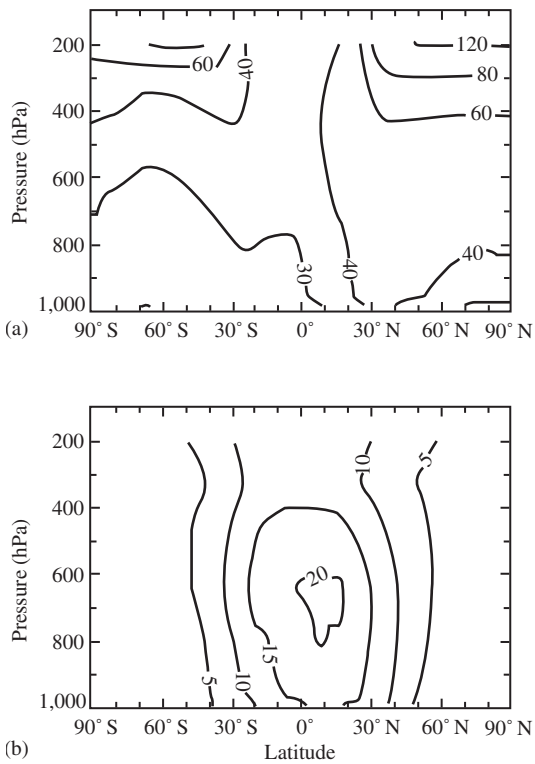

Figure 1 (a) Ozone mole fractions (in ppb) and (b) hydroxyl radical concentrations (in 10^5 radicals cm^{-3}) as functions of latitude and pressure (in hPa) from a model of the atmosphere in the 1990s (source Wang and Jacob, 1998).

Because O_3 is a powerful infrared absorber and emitter (a "greenhouse" gas), and because many other greenhouse gases, notably CH_4, are destroyed principally by reaction with OH, there are significant connections between atmospheric oxidation processes and climate. Added to these greenhouse gas related connections is the fact that the first step in the production of aerosols from gaseous SO_2, NO_2, and hydrocarbons is almost always the reaction with OH. Aerosols play a key role in climate through absorption and/or reflection of solar radiation.

These oxidation processes also dominate in the chemistry of air pollution, where the occurrence of harmful levels of O_3 and acidic aerosols depends on the relative and absolute levels of urban emissions of NO, CO, RH, and SO_2. In the marine and polar troposphere, reactive compounds of chlorine, bromine, and iodine provide a small but significant additional pathway for oxidation besides OH, as discussed by von Glasow and Crutzen (see Chapter 4.02).

This chapter reviews the possible evolution of oxidizing capacity over geologic time, the fundamental chemical reactions involved, and the influences of meteorology and human activity on atmospheric oxidation. The measurement of oxidation rates (i.e., oxidative capacity), and the complex interactive models of chemistry, transport, and human and other biospheric activities that are now being developed to help understand atmospheric oxidation as a key process in the Earth system are also discussed.

4.01.2 EVOLUTION OF OXIDIZING CAPABILITY

A discussion of the evolution of O_3 and OH over geologic time needs to be placed in the context of the evolution of the Earth system (see Table 3). The Earth accreted between 4.5 and 4.6 billion years (Gyr) before present (BP). Enormous inputs of kinetic energy, ice, and hydrated minerals during accretion would have led to a massive H_2O (steam) atmosphere with extremely high surface temperatures (Lange and Ahrens, 1982). This earliest atmosphere may also have been partly or largely removed by the subsequent Moon-forming giant impact. Due to the apparent obliteration of rocks much older than 4 Gyr on Earth, very little is known directly

Table 3 Schematic showing time in billions of years before present, major eras and associated biospheric and geospheric evolutionary events, and hypothesized atmospheric composition. Gases are listed in order of their hypothesized concentrations and those whose sources and/or sinks are dominated by biological processes are denoted with an asterisk. Note the transition from an abiotic to an essentially biologically controlled atmosphere over geologic time.

Time (Gyr BP)	*Major evolutionary events*	*Hypothesized atmospheric compositions*
	Earth accretes and massive steam atmosphere forms	[H_2O, CO_2, CO, N_2, H_2]
	Surface cools, volcanism begins?	
	Ocean forms, continental weathering, and carbonate precipitation begin	[CO_2, CO, N_2, H_2O, H_2]
4	Archean era begins, oldest rocks	
	Late heavy bombardment	
	Sediment subduction and volatile recycling begins?	[N_2, CO_2, CO, H_2O, H_2, CH_4, HCN, NO_x]
	First living organisms evolve, prokaryotes	
3	First protosynthetic organisms evolve: cyanobacteria, stromatolites	[N_2, H_2O, CO_2, $*O_2$, CH_4]
	Proterozoic era begins: scarce fossils	
2	Aerobic biosphere with nitrogen and methane microbes evolves	[$*N_2$, $*O_2$, H_2O, $*CO_2$, $*CH_4$, $*N_2O$]
1	Eucaryotes evolve	
	Metazoans appear	
	Invertebrates appear	
	Paleozoic era begins, ubiquitous fossils	
	Fishes appear	[$*N_2$, $*O_2$, H_2O, $*CO_2$, $*CH_4$, $*N_2O$]
	Land plants appear	
	Amphibians appear	
	Mesozoic (reptilian) era begins	
	Fission of Pangean supercontinent	
	Cretaceous–Tertiary collision	
	Cenozoic (mammalian) era begins	
0	Present	[$*N_2$, $*O_2$, H_2O, $*CO_2$, $*CH_4$, $*N_2O$, $*CF_2Cl_2$, etc.]

about the Earth's earliest atmosphere. It is hypothesized that, as the Earth cooled, the massive H_2O atmosphere condensed forming oceans and a much less massive $CO_2/CO/N_2/H_2O/H_2$ atmosphere then evolved.

The next big evolutionary step, involving the aqueous weathering of rocks and removal of CO_2 as carbonates, had occurred ~3.8 Gyr ago (Holland, 1984). Thus, the early Archaean atmosphere was probably largely dominated by N_2 with smaller amounts of CO_2, CO, H_2O, H_2, CH_4, HCN, and NO_x (from lightning). The evolution of the first life forms (procaryotes), and specifically photosynthetic cyanobacteria, would have allowed the slow accumulation of biologically produced O_2 in the atmosphere in the late Archaean period. Similarly, the early evolution of methane and nitrogen bacteria along with the evolution of the aerobic biosphere led, apparently early in the Proterozoic, to an $N_2/O_2/H_2O/CO_2/CH_4/N_2O$ atmosphere with all of these gases, with the exception of H_2O, being largely controlled by biological sources and biological or atmospheric chemical sinks.

4.01.2.1 Prebiotic Atmosphere

Before the evolution of the photosynthetic source of O_2, the atmosphere was relatively chemically neutral or even reducing. Its reduction state would have depended significantly on the quantities of reduced gases produced from volcanic sources (e.g., sources in which primordial iron, sulfur, carbon, and organic compounds were thermally oxidized by H_2O and CO_2 producing H_2, CO, and CH_4 (Prinn, 1982; Lewis and Prinn, 1984)). In these prebiotic atmospheres, small amounts of O_2 can be produced from H_2O photodissociation (Levine, 1985), and small quantities of NO can be formed by shock heating, by lightning, and large collisions (Chameides and Walker, 1981; Prinn and Fegley, 1987; Fegley *et al.*, 1986).

However, it is reasonable to conclude that the evolution of the powerful oxidizing processes involving O_3 and OH in the present atmosphere had to await the evolution of photosynthetic O_2. Before that, atmospheric chemical transformations were probably driven by simple photodissociation

and dissolution reactions and by episodic processes like lightning and collisions. The transformation from reducing/neutral to oxidizing atmosphere was itself a long-term competition between abiotic sources of reduced gases, anaerobic microbial processes, and finally the aerobic biological processes which came to dominate the biosphere. Once the land biosphere evolved, the burning of vegetation ignited by lightning provided an additional source of trace gases (see Chapter 4.05).

4.01.2.2 Pre-industrial Atmosphere

We expect that OH and O_3 changed even under the approximately constant levels of atmospheric O_2 in the Cenozoic era. For example, the glacial–interglacial cycles should have significantly changed atmospheric H_2O (inferred to be low in ice ages) and CH_4 (observed to be low in ice ages). But these particular changes would have partially offsetting effects on OH (by lowering both OH production and OH removal rates in ice ages). And unfortunately, the lack of direct information about the abundance of the key short-lived gases (CO, NO_x, nonmethane hydrocarbons (NMHC), and stratospheric O_3) in paleoenvironments make it difficult to be quantitative about past OH changes (Thompson, 1992). One observational record over the past millennium which is useful in this respect is the analysis of hydrogen peroxide (H_2O_2) in Greenland permafrost, which indicates stable H_2O_2 from the years 1300 to 1700 followed by a 50% increase through to 1989 (however, most of the increase has occurred since 1980 and is not seen in Antarctic permafrost (Sigg and Neftel, 1991; Anklin and Bales, 1997)).

Increases in H_2O_2 during industrialization could signal a decrease in OH due to net conversion of HO_2 to H_2O_2 rather than recycling of HO_2 back to OH. Staffelbach *et al.* (1991) have used CH_2O measurements in Greenland ice cores to suggest that pre-industrial OH levels were 30% higher than the levels in the late twentieth century. Indeed, a variety of model studies which assume low pre-industrial emissions of CO, NO_x, and NMHC compared to the levels in the twentieth century suggest that the OH levels in the years 1200–1800 were ~10–30% higher than the levels at the end of the twentieth century (Thompson, 1992). Ozone levels in the 1880s can be inferred from iodometric measurements (Volz and Kley, 1988; Marenco *et al.*, 1994) indicating mole fractions as low as $(7-12)\times10^{-9}$, which are lower by a factor of 3 or more from those observed in the 1990s. Such low levels of O_3 are difficult to reconcile with CO measurements in ice cores (Haan *et al.*, 1996) indicating CO mole fractions of $\sim60\times10^{-9}$ (Antarctica) and $\sim90\times10^{-9}$ (Greenland), which are not much less than those observed today. As we will discuss in Section 4.01.3.1, oxidation of each CO molecule ought to produce one O_3 molecule, so that presuming OH levels in the 1880s to be similar to those in the 1990s implies similar O_3 production rates from CO.

4.01.3 FUNDAMENTAL REACTIONS

4.01.3.1 Troposphere

As we noted in Section 4.01.1, the ability of the troposphere to chemically transform and remove trace gases depends on complex chemistry driven by the relatively small flux of energetic solar UV radiation that penetrates through the stratospheric O_3 layer (Levy, 1971; Chameides and Walker, 1973; Crutzen, 1979; Ehhalt *et al.*, 1991; Logan *et al.*, 1981; Ehhalt, 1999; Crutzen and Zimmerman, 1991). This chemistry is also driven by emissions of NO, CO, and hydrocarbons and leads to the production of O_3, which is one of the important indicators of the oxidizing power of the atmosphere. But the most important oxidizer is the hydroxyl free radical (OH), and a key measure of the capacity of the atmosphere to oxidize trace gases injected into it is the local concentration of hydroxyl radicals.

Figure 2 summarizes, with much simplification, the chemistry involved in production and removal of O_3 and OH (Prinn, 1994). This chemistry is remarkable because it involves compounds that also influence climate, air pollution, and acid rain.

The greenhouse gases involved here include H_2O, CH_4, and O_3. Primary pollutants emitted mainly as a result of human activity (including fossil-fuel combustion, biomass burning, and land-use) include RH, CO, and nitrogen oxides (NO, NO_2). Reactive free radicals or atoms are in two categories: the very reactive species, such as $O(^1D)$ and OH, and the less reactive ones, such as HO_2, $O(^3P)$, NO, and NO_2.

The atmospheric cleansing role of OH is very evident in Figure 2. When OH reacts with an RH, the latter is oxidized in a series of steps mostly to CO. These steps consume OH but may also produce HO_2. In turn, OH oxidizes CO to CO_2, and it also oxidizes the gases NO_2 and SO_2 to nitric (HNO_3) and sulfuric (H_2SO_4) acids, respectively. The primary OH source involves water vapor which reacts with the very reactive singlet oxygen atom, $O(^1D)$, that comes from photodissociation of O_3 by solar UV radiation at wavelengths less than 310 nm. Typically, OH within a second of its formation oxidizes other compounds either by donating oxygen or by

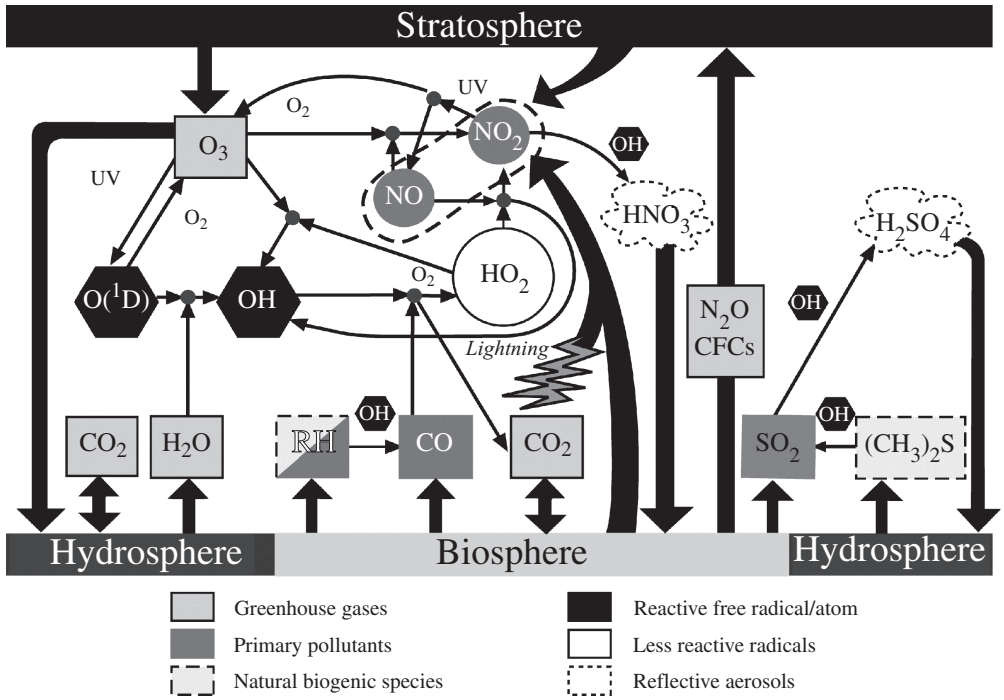

Figure 2 Schematic showing principle oxidation processes in the troposphere in NO_x-rich air (after Prinn, 1994). In NO_x-poor air (e.g., remote marine air), recycling of HO_2 to OH is achieved by reactions of O_3 with HO_2 or by conversion of $2HO_2$ to H_2O_2 followed by photodissociation of H_2O_2. In a more complete schematic, nonmethane hydrocarbons (RH) would also react with OH to form acids, aldehydes and ketones in addition to CO.

removing hydrogen leaving an H atom or organic free radical (R). Then R and H attach rapidly to molecular oxygen to form hydroperoxy radicals (HO_2) or organoperoxy radicals (RO_2), which are relatively unreactive. If there is no efficient way to rapidly recycle HO_2 back to OH, then levels of OH are kept low.

Adding the nitrogen oxides (NO and NO_2), which have many human-related sources, significantly changes this picture. Specifically, NO reacts with the HO_2 to form NO_2, and reform OH. UV radiation then decomposes NO_2 at wavelengths less than 430 nm to form O_3 and reform NO, so the nitrogen oxides are not consumed in this reaction. In a study of relatively polluted air in Germany, Ehhalt (1999) estimated that the production rate of OH by this secondary path involving NO is 5.3 times faster than the above primary path involving $O(^1D)$. Note that the reaction of NO with HO_2 does not act as a sink for the so-called odd hydrogen (the sum of the H, OH, and HO_2 concentrations). Rather, it determines the ratio of OH to HO_2. In the Ehhalt (1999) study, the $[HO_2]:[OH]$ ratio was 44 : 1. This is due to, and indicative of, the much greater reactivity of OH compared to HO_2. To summarize, the principal catalyzed reactions creating OH and O_3 in the troposphere are shown in Equations (1)–(3), (4)–(9), and (10)–(15):

$$O_3 + UV \rightarrow O_2 + O(^1D) \quad (1)$$

$$O(^1D) + H_2O \rightarrow 2OH \quad (2)$$

$$\text{Net effect: } O_3 + H_2O \rightarrow O_2 + 2OH \quad (3)$$

and

$$OH + CO \rightarrow H + CO_2 \quad (4)$$

$$H + O_2 \rightarrow HO_2 \quad (5)$$

$$HO_2 + NO \rightarrow OH + NO_2 \quad (6)$$

$$NO_2 + UV \rightarrow NO + O \quad (7)$$

$$O + O_2 \rightarrow O_3 \quad (8)$$

$$\text{Net effect: } CO + 2O_2 \rightarrow CO_2 + O_3 \quad (9)$$

and

$$OH + RH \rightarrow R + H_2O \quad (10)$$

$$R + O_2 \rightarrow RO_2 \quad (11)$$

$$RO_2 + NO \rightarrow RO + NO_2 \quad (12)$$

$$NO_2 + UV \rightarrow NO + O \quad (13)$$

$$O + O_2 \rightarrow O_3 \quad (14)$$

$$\text{Net effect: } OH + RH + 2O_2 \rightarrow RO + H_2O + O_3 \quad (15)$$

In theoretical models, the global production of tropospheric O_3 by the above pathway beginning with CO is typically about twice that beginning with RH. For most environments, it is these overall catalytic processes that pump the majority of the OH and O_3 into the system. If the concentration of NO_2 becomes too high, however, its reaction with OH to form HNO_3 ultimately limits the OH concentration (see Section 4.01.4). The global impact of the above tropospheric OH production mechanisms has been summarized in Table 2. Hough and Derwent (1990) have estimated the global production rate of tropospheric O_3 by the above reactions to be 2,440 Tg yr^{-1} in pre-industrial times and 5,130 Tg yr^{-1} in the 1980s with the increase caused by man-made NO_x, hydrocarbons, and CO.

An update to the above 1980s calculation (Ehhalt, 1999) gives a production rate of 4,580 Tg yr^{-1}. A comparison of several tropospheric O_3 models showed a chemical production rate range for O_3 of 3,425–4,550 Tg yr^{-1} (Lelieveld *et al.*, 1999). Since the troposphere contains ~350 Tg of O_3 (Ehhalt, 1999), the chemical replenishment time for O_3 (defined as the tropospheric content divided by the tropospheric chemical production rate) is 28–37 d. This is much longer than the replenishment time for OH, ~1 s, and indicates the enormous reactivity of OH relative to O_3.

How stable is the oxidizing capability of the troposphere? How might it have changed over geologic time even after oxygen reached near today's levels? If emissions of gases that react with OH such as CH_4, CO, and SO_2 are increasing then, keeping everything else constant, OH levels should decrease. Conversely, increasing NO_x -emissions from combustion (of biomass in the past (see Chapter 4.05) augmented by fossil fuel today) should increase tropospheric O_3 (and thus the primary source of OH), as well as increase the recycling rate of HO_2 to OH (the secondary source of OH).

Also, if the temperatures of oceans are increasing, we expect increased water vapor in the lower troposphere. Because water vapor is part of the primary source of OH, climate warming also increases OH. This increase could be lowered or raised due to changes in cloud cover accompanying the warming leading to more or less reflection of UV back toward space. Rising temperature also increases the rate of reaction of CH_4 with OH, thus lowering the lifetimes of both chemicals. The opposite conclusions apply if trace gas emissions increase or the climate cools. Finally, decreasing stratospheric O_3 can also increase tropospheric OH.

4.01.3.2 Stratosphere

The O_3 in the stratosphere is maintained by a distinctively different set of chemical reactions than the troposphere. The flow diagram in Figure 2 shows how the driving chemicals like water vapor, chlorofluorocarbons, and nitrous oxide, are transported up from the troposphere to the stratosphere, where they produce chlorine-, nitrogen-, and hydrogen-carrying free radicals, which destroy O_3. There is an interesting paradox here: the nitrogen oxide free radicals, which are responsible for destroying a significant fraction of the O_3 in the stratosphere, are the same free radicals that are producing O_3 in the troposphere through the chemistry outlined earlier (Figure 3).

When the ratio of nitrogen oxide free radicals to O_3 is low, as it is in the stratosphere, the net effect is for O_3 to be destroyed overall, while if this ratio is high, as it is in much of the troposphere, then O_3 is produced overall (Crutzen, 1979).

The stratosphere is chemically very active due to its high O_3 and UV levels. But the densities and usually temperatures are much lower than in the lower troposphere so that only a small fraction of the destruction of the gases listed in Table 2 occurs in the stratosphere. The stratosphere contains ~90% of the world's O_3 and exports ~400–846 Tg yr^{-1} of O_3 to the troposphere to augment the chemical production discussed in Section 4.01.3.1 (Lelieveld *et al.*, 1999).

There is also an important link between stratospheric chemistry and climate. The precursor gases for the destructive free radicals in the stratosphere are themselves greenhouse gases, as is the stratospheric O_3 itself. Therefore, while increases in the concentrations of the source gases will increase the radiative forcing of warming, these increases will, at the same time, lead to decreases in stratospheric O_3, thus lowering the radiative forcing. Once again, as in the troposphere, there are important feedbacks

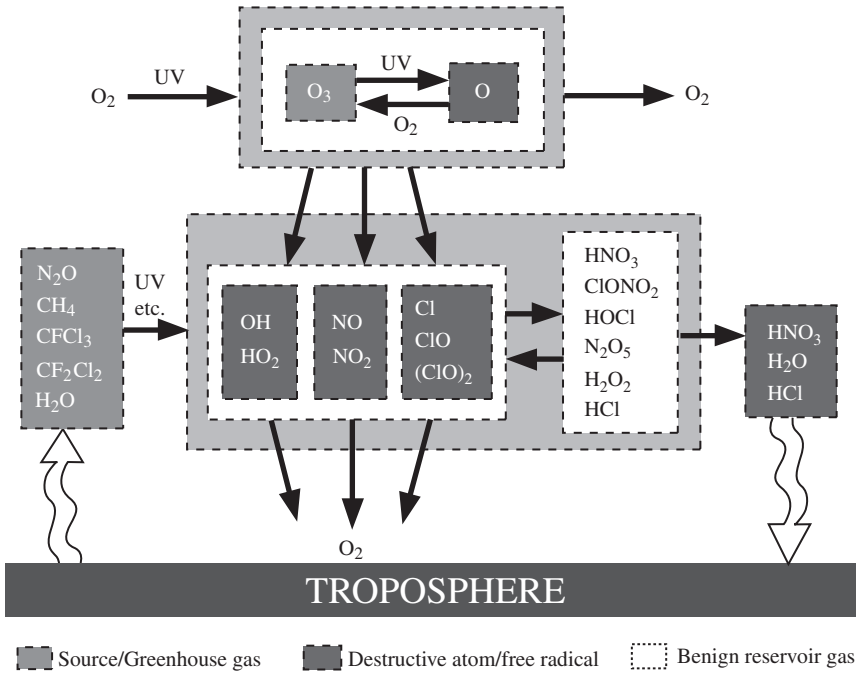

Figure 3 Schematic showing major chemical processes forming and removing O_3 in the stratosphere (after Prinn, 1994). UV photodissociaton of largely natural (N_2O, CH_4, H_2O) and exclusively man-made ($CFCl_3$, CF_2Cl_2) source gases leads to reactive HO_x, NO_x, and ClO_x free radicals which catalytically destroy O_3. The catalysts reversibly form reservoir compounds (HNO_3, etc.), some of which live long enough to be transported down to the troposphere.

between chemical processes and climate through the various greenhouse gases. It is not just man-made chemicals that can change the stratospheric O_3. Changes in natural emissions of N_2O and CH_4, and changes in climate that alter H_2O flows into the stratosphere, undoubtedly led to changes in the thickness of the O_3 layer over geologic time even after O_2 levels reached levels near those in the early 2000s.

There is also a strong link between the thickness of the stratospheric O_3 layer and concentrations of OH in the troposphere. Because $O(^1D)$ can only be produced from O_3 at wavelengths less than 310 nm, and the current O_3 layer effectively absorbs all incoming UV at less than 290 nm, there is only a very narrow window of 290–310 nm radiation that is driving the major oxidation processes in the troposphere. Decrease in the amount of stratospheric O_3, which has occurred since about 1980, can therefore increase the tropospheric OH by increasing the flux of radiation less than 310 nm which reaches the troposphere to produce $O(^1D)$ (Madronich and Granier, 1992). By the same arguments, if the stratospheric O_3 layer was very much thicker in the past, it would have removed a great deal of the "cleansing" capacity of the Earth's troposphere leading to much higher levels of gases like CO and CH_4.

4.01.4 METEOROLOGICAL INFLUENCES

The oxidative capability of the atmosphere is not simply a function of chemistry. Convective storms can carry short-lived trace chemicals from the planetary boundary layer (the first few hundred to few thousand meters) to the middle and upper troposphere in only a few to several hours. This can influence the chemistry of these upper layers in significant ways by delivering, e.g., reactive hydrocarbons to high altitudes. Conversely, the occurrence of very stable conditions in the boundary layer can effectively trap chemicals near the surface for many days, leading to polluted air. Larger-scale circulations serve to carry gases around latitude circles on timescales of a few weeks, between the hemispheres on timescales of a year, and between the troposphere and stratosphere on timescales of a few years.

A convenient measure of the stability of a trace chemical is its local chemical lifetime, which is defined as its local concentration (e.g., in mol L^{-1}) divided by its local removal rate (e.g., in mol L^{-1} s^{-1}). Concentrations of chemicals whose lifetimes (due to chemical destruction or deposition) are comparable to, or longer than, the above transport times will be profoundly affected by transport. As a simple example, in a steady (constant concentration) state with a horizontal

wind u, the concentration $[i]$ of chemical i whose lifetime is t_i decreases downwind of a source region (located at horizontal position $x = 0$) according to

$$[i](x) = [i](0)\exp\left[\frac{-x}{(ut_i)}\right]$$

Specifically, the concentration of i decreases by a factor of e over the distance scale ut_i. Note also that, if the transport time x/u is much less than t_i, the concentration remains essentially constant and the species can be considered to be almost inert. For oxidation by OH of NO_2 and SO_2 to form the acids HNO_3 and H_2SO_4, the time t_i is typically 3 d (2.6×10^5 s), so the e-folding distance ut_i is only ~800 km for a typical u of 3 m s^{-1}. Alternatively, for the oxidation of CO by OH to form CO_2, $t_i = 3$ months (7.9×10^6 s), so $ut_i = 2.4 \times 10^4$ km for the same u. In a simple way this illustrates why NO_2 and SO_2 are local or regional pollutants, whereas CO is a hemispheric pollutant.

In the above example, if the chemical lifetime t_i is much less than the transport time x/u then we could ignore transport and simply consider chemical sources and sinks to determine concentrations. However, for the chemicals controlling oxidation reactions, care must be taken in defining t_i. Specifically, sometimes members of a "chemical family" are converted from one to another on very short timescales relative to transport, whereas the total population of the family is produced and removed on longer timescales.

For example, in the family composed of NO and NO_2 (called the NO_x family) the reactions shown in Equations (16)–(18) rapidly interconvert NO and NO_2 on timescales much less than typical transport times and do so without affecting the total $[NO_x] = [NO] + [NO_2]$.

$$NO + O_3 \rightarrow NO_2 + O_2 \quad (16)$$

$$NO_2 + h\nu \rightarrow NO + O \quad (17)$$

$$O + O_2 + M \rightarrow O_3 + M \quad (18)$$

$$NO_2 + OH + M \rightarrow HNO_3 + M \quad (19)$$

However, the removal of NO_x by the reaction shown in Equation (19) is much slower (e.g., ~3 d). Thus, we can use the chemical steady-state approximation (which equates chemical production to chemical loss only) to define the ratio of NO to NO_2. We must however take full account of transport in calculating $[NO_x]$. Similar arguments hold for the "odd oxygen" ($[O_x] = [O] + [O_3]$) and "odd hydrogen" ($[HO_x] = [H] + [OH] + [HO_2]$) families.

Besides being a vigorous vertical transport mechanism, moist convection also directly affects the oxidizing reactions in the atmosphere. First, lightning and thundershocks serve to thermally convert atmospheric N_2 and O_2 to 2NO, leading to a very important natural source of NO_x. Second, the formation of cloud droplets is aided by (and consumes) aerosols (as cloud condensation nuclei), and the cloud droplets then serve as sinks for soluble species like H_2O_2, HNO_3, NO_x, SO_2, and H_2SO_4. For some oxidation reactions, e.g., oxidation of SO_2 to H_2SO_4, this dissolution leads to an additional nongaseous pathway for oxidation generally considered comparable to the gas-phase processes for SO_2. Finally, the formation of convective clouds, and particularly the extensive anvils, leads to reflection of UV radiation enhancing the photo-oxidation processes above the cloud and inhibiting them below (e.g., Wang and Prinn, 2000).

4.01.5 HUMAN INFLUENCES

4.01.5.1 Industrial Revolution

The advent of industrialization since 1850 has led to significant increases in the global emissions of NO_x, CO, NMHC, and CH_4 (Wang and Jacob, 1998; Prather *et al.*, 2001). Biomass burning associated with human land use provides an additional source of these trace gases (see Chapter 4.05). Also, the observed temperature increase of 0.6 ± 0.2 °C in this time period (Folland *et al.*, 2001) should have led to increases in tropospheric H_2O and possibly changes in global cloud cover (of unknown sign). Anthropogenic aerosols, both scattering and absorbing, have also increased due to human activity (Penner *et al.*, 2001). These aerosol increases should decrease UV fluxes below the cloud tops due to both their direct optical effects (absorbing or reflecting) and their indirect effects as cloud condensation nuclei, which should increase the reflectivity of water clouds. Finally, depletion of stratospheric O_3, which has occurred due to man-made halocarbons, will increase tropospheric UV irradiation (Madronich and Granier, 1992).

All of these changes should have affected O_3 and OH concentrations, sometimes offsetting and sometimes augmenting each other, as discussed earlier. Table 4 summarizes the expected changes in OH and O_3 relative to pre-industrial times. Where quantitative estimates are not available, only the signs of expected changes are indicated. Note in particular that for OH the positive effects of NO_x increases have been more than offset by the negative effects of CO, NMHC, and CH_4 increases, so the net change in OH is a modest 10% decrease (Wang and Jacob, 1998; see also Levy *et al.*, 1997).

Table 4 Effects of anthropogenically driven or observed changes in trace gas emissions, concentrations, or meteorological variables between pre-industrial and present times on the oxidizing capability of the atmosphere (expressed where available as percentage changes (Δ) in [OH] or [O_3] from pre-industrial to present).

	Present/pre-industrial	*Δ[OH]/[OH]*	*Δ[O_3]/[O_3]*
NO_x[a]	4.7	+36%	+30%
CO[a]	3.2	−32%[b]	+10%[b]
NMHC[a]	1.6		
CH_4[a]	2.1	−17%	+13%
Combined[a]		−10%[c]	+63%[c]
H_2O(T)	>1	>0	>0
Clouds[d]	>1, <1	<0, >0	<0, >0
Scat. aero[e]	>1	<0	<0
Abs. aero[f]	>1	<0	<0
Strat. O_3[g]	<1	>2%	>0

[a] Wang and Jacob (1998). Individual effect of each specific chemical computed in sensitivity runs with pre-industrial conditions except for the specific chemical which is at present levels. [b] CO and NMHC effects combined. [c] CO, NMHC, CH_4, and NO_x effects combined. Total effect not equal to sum of individual effects due to interactions. [d] Cloud cover changes unknown. Effects shown for either an increase or a decrease. [e] Specifically aerosols with high single scattering albedos (e.g., sulfates) which reflect UV radiation back to space. [f] Specifically aerosols with low single scattering albedos (e.g., black carbon) which absorb UV radiation. [g] Madronich and Granier (1992) and Krol *et al.* (1998).

Table 5 Percentages by which either emissions of NO_x, CO, NMHC (plus oxidized NMHC), and CH_4, or concentrations of tropospheric OH, or column amounts of tropospheric O_3, are projected to change between 2000 and 2100 for various IPCC scenarios.

Scenario	*NO_x* (%)	*CO* (%)	*NMHC* (%)	*CH_4* (%)	*OH* (%)	*O_3* (%)[a]
A1B	+26	+90	+37	−11	−10	+7.7
A1T	−12	+137	−9.2	−15	−18	+5.5
A1FI	+243	+193	+198	+128	−14	+47
A2	+241	+165	+143	+175	−12	+46
B1	−42	−59	−38	−27	+5	−8.6
B2	+91	+128	+21	+85	−16	+23
A1p	+27	+138	+15	−13	−18	+11
A2p	+238	+140	+133	+163	−12	+46
B1p	+3.4	−8.3	+2.0	+9.2	−3	+2.6
B2p	+86	+100	+13	+46	−11	+19
IS92a	+124	+64	+125	+95	−11	+29

Source: Prather *et al.* (2001).
[a]Ozone changes decreased by 25% to account for modeling errors as recommended by IPCC.

Since combustion is a common, and (except for CH_4) a dominant source for all these gases affecting OH, then the offsetting increases of NO_x, CO, and hydrocarbons mean that OH levels are not very sensitive overall to past increases in combustion. Note, however, that if future air pollution controls lower NO_x emissions more than CO and hydrocarbon emissions, then OH decreases should result.

For O_3, in contrast to OH, the effects of NO_x, CO, and RH emission increases are additive and in sum are calculated to have caused ~63% increase in O_3 (Wang and Jacob, 1998). The actual increase may be even larger, since observations (albeit not very accurate) of O_3 during the 1800s (Marenco *et al.*, 1994) suggest even lower values than those computed by Wang and Jacob (1998).

4.01.5.2 Future Projections

The importance of oxidation processes in climate led the Intergovernmental Panel on Climate Change (IPCC) to investigate the effects on O_3 and OH of 11 IPCC scenarios for future anthropogenic emissions of the relevant O_3 and OH precursors (Prather *et al.*, 2001). In all of the scenarios, except one, OH was projected to decrease between 2000 and 2100 by 3–18%, while O_3 was projected to increase by 2.6–46% (Table 5). The smallest decrease in OH and smallest increase in O_3 was seen as expected in the scenario in which emissions of NO_x, CO, NMHCs, and CH_4 were projected to change by only +3.4%, −8.3%, +2.0%, and +9.2%, respectively, between 2000 and 2100. Also as expected, the greatest OH decreases were seen in two

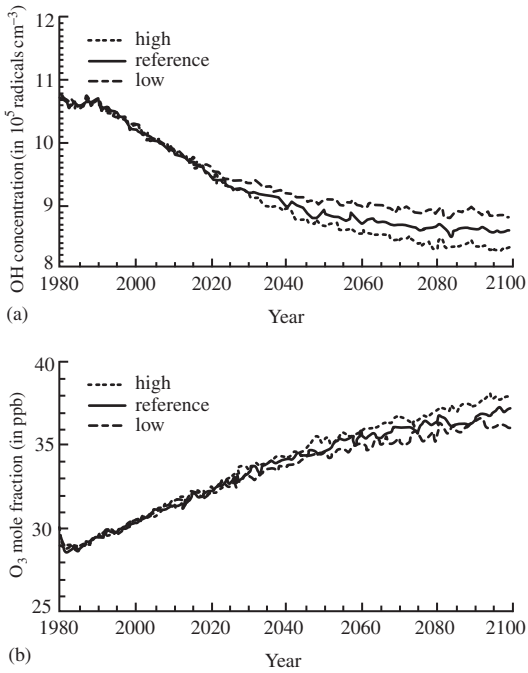

Figure 4 (a) Predicted future tropospheric average concentrations of OH and (b) mole fractions of O_3 for three scenarios of future emissions of O_3 and OH precursors (as well as greenhouse gases) predicted in an economics model (Prinn *et al.*, 1999). The natural system model receiving these emissions includes simultaneous calculations of atmospheric chemistry and climate (Wang and Prinn, 1999).

scenarios in which small increases or even decreases in NO_x emissions (OH source) were accompanied by relatively very large increases in CO emissions (OH sink). The greatest O_3 increases were seen in two scenarios where emissions of all four O_3 precursors increased very substantially. Finally, the one anomalous scenario (in which OH increased by 5% and O_3 decreased by 8.6%) involved significant decreases in emissions of all four precursors (which is very unlikely).

The above results make it very clear that forecasts of the future oxidation capacity of the atmosphere depend critically on the assumed emissions. The IPCC did not assign probabilities to its emission scenarios but it is apparent that some of these scenarios are highly improbable for oxidant precursor emissions. Integrated assessment models, which couple global economic and technological development models with natural Earth system models provide an alternative approach to the IPCC scenario approach with the added advantage that objective estimates of individual model uncertainties can be combined with Monte Carlo approaches to provide more objective ways of defining means and errors in forecasts. We will use here one such model (Prinn *et al.*, 1999) that integrates a computable general equilibrium economics model with a coupled chemistry and climate model, and an ecosystem model. The economics model automatically accounts for the strong correlations between emissions of air pollutants (gases and aerosols) and greenhouse gases due to their common production processes (e.g., combustion of coal, oil, gasoline, gas, biomass).

Results from this model for (i) a high-probability reference emissions forecast and (ii) a lower-probability high and low emissions forecasts are shown in Figure 4 (Wang and Prinn, 1999). Emissions driving these projections are summarized in Prinn *et al.* (1999); reference anthropogenic CO, NO_x, and CH_4 emissions increase by ~18%, ~95%, and ~33%, respectively, between 2000 and 2100 in these projections. Evidently, these emission projections from the economics model (which consistently models all of the relevant industrial and agricultural sectors producing these gases) lead to projections of significant depletion of OH and enhancement of O_3 between 2000 and 2100 with magnitudes comparable to the larger of the changes predicted from the IPCC scenarios (Table 5).

4.01.6 MEASURING OXIDATION RATES

Given its importance as the primary oxidizing chemical in the atmosphere, a great deal of effort has been given to measuring OH concentrations and trends. Two approaches, direct and indirect, have been taken to address this measurement need.

4.01.6.1 Direct Measurement

The direct accurate measurement of local OH concentrations has been one of the major technical challenges in atmospheric chemistry since the early 1980s. This goal was first achieved in the stratosphere (e.g., Stimpfle and Anderson, 1988), but the troposphere proved more difficult (Crosley, 1995). Nevertheless, early long-baseline absorption methods for OH were adequate to test some basic theory (e.g., Poppe *et al.*, 1994). Current successful direct methods include differential optical absorption near-UV spectroscopy with long baselines (e.g., Mount, 1992; Dorn *et al.*, 1995; Brandenburger *et al.*, 1998), laser-induced fluorescence after expansion of air samples (e.g., Hard *et al.*, 1984, 1995; Holland *et al.*, 1995), and a variety of chemical conversion techniques (Felton *et al.*, 1990; Chen and Mopper, 2000; Tanner *et al.*, 1997).

The long-baseline spectroscopic techniques require path lengths in air of 3–20 km, which

can be achieved by a single pass through air (e.g., Mount and Harder (1995) used a 10.3 km path to achieve a sensitivity of 5×10^5 radicals cm^{-3}), or multiple reflections in long cells (e.g., Dorn *et al.* (1995) used 144 passes through a 20 m cell to observe six OH absorption lines around 308 nm). The laser-induced fluorescence methods use either 282 nm or 308 nm photons to excite OH, which then subsequently emits at 308–310 nm (e.g., Brune *et al.* (1995); Holland *et al.* (1995) use 308 nm laser light and achieve detection limits of $(1-3) \times 10^5$ radicals cm^{-3}).

The common chemical conversion techniques use a flow reactor in which ambient OH reacts with isotopically labeled SO_2 or CO to yield observable products (e.g., Felton *et al.* (1990) used ^{14}CO with radioactive $^{14}CO_2$ detection, while Eisele and Tanner (1991) used $^{34}SO_2$ with $H_2\,^{34}SO_4$ detection by ion-assisted mass spectrometry).

These various direct OH measurement techniques enable critical tests of current theoretical models of fast photochemistry. This is achieved by simultaneously measuring NO, NO_2, CO, H_2O, O_3, RH, and other relevant trace species, UV fluxes, the frequency of photodissociation of O_3 to produce $O(^1D)$, and the concentrations of OH (and sometimes HO_2). A model incorporating the best estimates of the relevant kinetic rate constants and absorption coefficients is then used, along with the trace gas and photodissociation rate measurements, to predict OH concentrations for comparison with observations. Examples of results from the Mauna Loa Observatory Photochemistry Experiment (MLOPEX) and the Photochemistry of Plant-emitted Compounds and OH Radicals in North Eastern Germany Experiment (POPCORN) are shown in Figures 5 and 6, respectively.

The 1992 MLOPEX experiment was able to sample both free tropospheric air (associated with downslope winds at this high mountain station) and boundary layer air (upslope winds). It is evident from Figure 5 that agreement between observed (using the $^{34}SO_2$ method) and calculated OH concentrations was always good in the free troposphere, but in the summer the calculated boundary layer OH was about twice that observed (Eisele *et al.*, 1996). Since the measurement accuracy was argued to be much better than factor of 2, this suggests a missing OH sink in their model, which they suggest might be due to unmeasured hydrocarbons from vegetation or undetected oxidation products of anthropogenic compounds.

The 1994 POPCORN experiment in rural Germany compared OH measurements using laser-induced fluorescence to calculations in a regional air chemistry model. Figure 6(a) shows the measured OH concentrations as a function

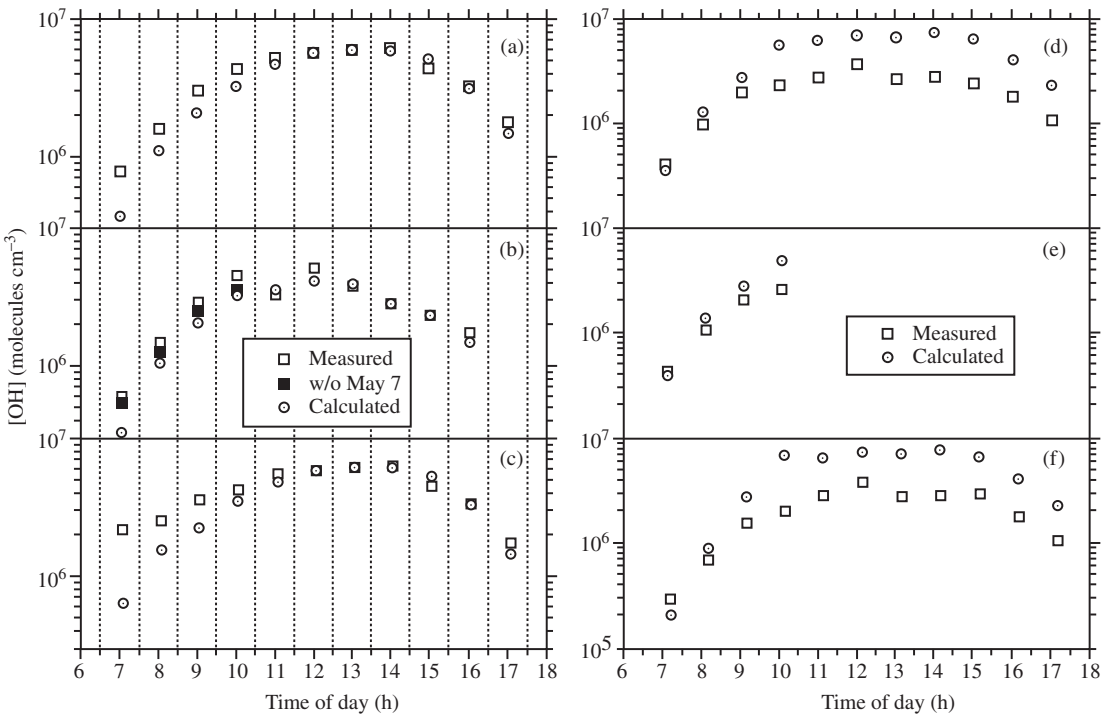

Figure 5 Hourly average measured and calculated OH concentrations during spring (a)–(c) and summer (d)–(f) of 1992 in MLOPEX: (a), (d) all time; (b), (e) free tropospheric air only; (c), (f) boundary layer air only (after Eisele *et al.*, 1996). May 7 measurements were anomalous.

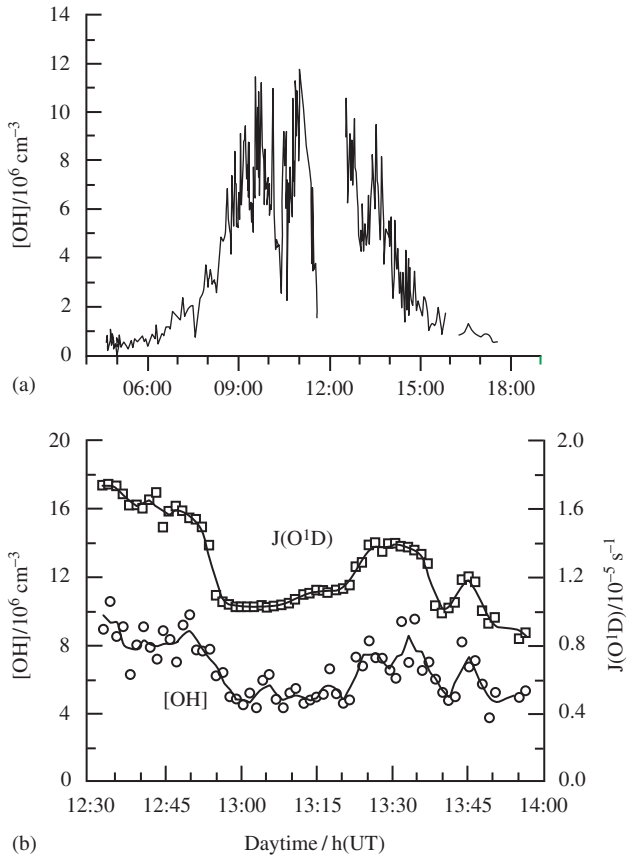

Figure 6 (a) Diurnal variation of OH concentrations during POPCORN (August 16, 1994) and (b) higher time resolution version of (a) showing fast response of OH concentrations to $J(O^1D)$ variations (solid lines are three-point running averages) (after Hofzumahaus *et al.*, 1996).

of time. Note the expected strong diurnal variation in OH due to the daily cycle in UV radiation. Also shown in Figure 6(b) is a demonstration of the expected strong correlation between the measured frequency of photoproduction of $O(^1D)$ from $O_3(J(O^1D))$ and the measured OH (see Section 4.01.3.1). The strong high-frequency variations in OH evident in Figure 6(a) are real and are due to strongly correlated variations in solar UV fluxes caused by transient cloud cover. The agreement between observed and calculated OH was quite good in POPCORN but, as in MLOPEX, there was also a tendency for the model to overpredict OH (Hofzumahaus *et al.*, 1996; Ehhalt, 1999). Part of the discrepancy may be attributable to the combined effects in the modeling of rate constant errors and measurement errors in the observed RH, CO, NO, NO_2, O_3, and H_2O used in the model. Poppe *et al.* (1995) have estimated this modeling error to be $\pm 30\%$.

Overall, considering the difficulties in both the measurements and the models, the agreements between observation and theory are encouraging at least for the relatively clean and clear air environments investigated in these experiments.

The power and great importance of the *in situ* direct measurement is that in conjunction with simultaneous *in situ* observations of the other components of the fast photo-oxidation cycles, they provide a fundamental test of the photochemical theory. However, the very short lifetime and enormous temporal and spatial variability of OH, already emphasized in Section 4.01.1, make it impossible practically to use these direct techniques to determine regional to global scale OH concentrations and trends. It is these large-scale averages that are essential to understanding the regional to global chemical cycles of all of the long-lived (more than a few weeks) trace gases in the atmosphere which react with OH as their primary sink. For this purpose, an indirect integrating method is needed.

4.01.6.2 Indirect Measurement

The large-scale concentrations and long-term trends in OH can in principle be measured indirectly using global measurements of trace

gases whose emissions are well known and whose primary sink is OH. The best trace gas for this purpose is the industrial chemical 1,1,1-trichloroethane (methylchloroform, CH_3CCl_3). First, there are accurate long-term measurements of CH_3CCl_3 beginning in 1978 in the ALE/GAGE/AGAGE network (Prinn *et al.*, 1983, 2000, 2001) and beginning in 1992 in the NOAA/CMDL network (Montzka *et al.*, 2000). Second, methylchloroform has fairly simple end uses as a solvent, and voluntary chemical industry reports since 1970, along with the national reporting procedures under the Montreal Protocol in more recent years, have produced very accurate emissions estimates for this chemical (McCulloch and Midgley, 2001).

Other gases which are useful OH indicators include ^{14}CO, which is produced primarily by cosmic rays (Volz *et al.*, 1981; Mak *et al.*, 1994; Quay *et al.*, 2000). While the accuracy of the ^{14}CO production estimates, and especially the frequency and spatial coverage of its measurements, do not match those for CH_3CCl_3, its lifetime (2 months) is much shorter than for CH_3CCl_3 (4.9 yr), so it provides estimates of average concentrations of OH that are more regional than CH_3CCl_3. Another useful gas is the industrial chemical chlorodifluoromethane (HCFC-22, $CHClF_2$). It yields OH concentrations similar to those derived from CH_3CCl_3 but with less accuracy due to greater uncertainties in emissions and less extensive measurements (Miller *et al.*, 1998). The industrial gases CH_2FCF_3 (HFC-134a), CH_3CCl_2F (HCFC-141b), and CH_3CClF_2 (HCFC-142b) are potentially useful OH estimators but the accuracy of their emission estimates needs improvement (Simmonds *et al.*, 1998; Huang and Prinn, 2002).

The most powerful methods for determining OH concentrations from trace gas data involve solution of an inverse problem in which the observables are expressed as Lagrangian line integrals, and the unknown OH concentrations (expressed as functions of space and time) are the integrands. The inverse problem of interest consists of determining an "optimal" estimate in the Bayesian sense of the unknown OH concentrations from imperfect concentration measurements of say CH_3CCl_3 over space and time. The unknown OH concentrations are arrayed in a "state" vector $\boldsymbol{x}^t$ and the CH_3CCl_3 measurement errors are arrayed in a "noise" vector. Approximating the line integral by a summation leads to the observed CH_3CCl_3 concentrations being expressed as the noise vector plus a matrix of "partial derivatives" ($\boldsymbol{H}$) multiplied by $\boldsymbol{x}^t$. $\boldsymbol{H}$ expresses the sensitivity of the chemical transport model (CTM) CH_3CCl_3 concentrations to changes in the state vector elements (i.e., to changes in OH). Given the discrete time series nature of CH_3CCl_3 measurements, it is convenient (but not essential) to solve for $\boldsymbol{x}^t$ using a discrete recursive optimal linear filter such as the discrete Kalman filter (DKF). The DKF has the specific useful property that it provides an objective assessment of the uncertainty in estimates of $\boldsymbol{x}^t$ as each CH_3CCl_3 measurement is used and thus of the usefulness of each measurement. Application of the DKF requires a CTM to compute $\boldsymbol{H}$.

While the derivation of the measurement equation uses Lagrangian concepts, $\boldsymbol{H}$ can be equally well derived using an Eulerian CTM. Several intuitive concepts exist regarding the important effects of observational errors and CTM errors on the value of the observations in improving and lowering the errors in the OH estimates (Prinn, 2000). (The latter paper is contained in a teaching monograph designed to introduce researchers to these inverse techniques applied to the biogeochemical cycles.) Application of optimal linear filtering requires careful attention to both the physics of the problem expressed in the "measurement" and "system" (or "state-space") equations or models, and the sources and nature of the errors in the observations and CTMs. This approach was the one adopted for analysis of CH_3CCl_3 data by the ALE/GAGE/AGAGE scientists from the inception of the experiment.

The use of CH_3CCl_3 has established that the global weighted average OH concentration in the troposphere is, over the 1978–2000 period, $\sim 10^6$ radicals cm^{-3} (Prinn *et al.*, 1987, 1992, 1995, 2001; Krol *et al.*, 1998; Montzka *et al.*, 2000). The weighting factor for this average is formally the rate constant k (which is temperature dependent) of the reaction of OH with methylchloroform, multiplied by the CH_3CCl_3 concentration, $[CH_3CCl_3]$. Practically, this means that the average is weighted toward the tropical lower troposphere. A similar average concentration is derived from ^{14}CO (Quay *et al.*, 2000), although the weighting here is not temperature dependent.

While the average OH concentration appears to be fairly well defined by this method, the temporal trends in OH are more difficult to discern since they require long-term measurements, and very accurate calibrations, model transports, and above all, a very accurate time series of CH_3CCl_3 emissions (Prinn *et al.*, 1992). In the first attempt at trend determination, Prinn *et al.* (1992) derived an OH trend of $1.0 \pm 0.8\%\ yr^{-1}$ between 1978 and 1990. Due primarily to a subsequent recalibration of the ALE/GAGE/AGAGE CH_3CCl_3 measurements, the estimated 1978–1994 trend was lowered to $0.0 \pm 0.2\%\ yr^{-1}$ (Prinn *et al.*, 1995). In a subsequent reanalysis of the same measurements (but not with the same emissions),

Krol *et al.* (1998) derived a trend of 0.46 ± 0.6% yr^{-1}. The reasons for this difference, including differences in models, data processing, emissions, and inverse methods, have been intensely debated (Prinn and Huang, 2001; Krol *et al.*, 2001). However, when the Prinn *et al.* (1995) method is used with the same emissions as Krol *et al.* (1998), it yields a trend of 0.3% yr^{-1}, in reasonable agreement with their value (Prinn and Huang, 2001).

In the latest analysis applied to the entire 1978–2000 ALE/GAGE/AGAGE CH_3CCl_3 measurements, Prinn *et al.* (2001) showed that global OH levels grew by 15 ± 22% between 1979 and 1989. But, the growth rate was decreasing at a statistically significant rate of 0.23 ± 0.18% yr^{-1}, so that OH began slowly declining after 1989 to reach levels in 2000 that were 10 ± 24% lower than the 1979 values (see Figure 7). Overall, the weighted global average OH concentration was $[9.4 \pm 1.3] \times 10^5$ radicals cm^{-3} with concentrations 14 ± 35% lower in the northern hemisphere than in the southern hemisphere. The Prinn *et al.* (2001) analysis included, in addition to the measurement errors, a full Monte Carlo treatment of model errors (transport, chemistry), emission uncertainties, and absolute calibration errors with the last two being the dominant contributors to OH trend errors.

Because these substantial variations in OH were not expected from current theoretical models, these results have generated much attention and scrutiny. Recognizing the importance of their assumed emissions estimates in their calculations, Prinn *et al.* (2001) also estimated the emissions required to provide a zero trend in OH. These required emissions differ by many standard deviations from the best industry estimates particularly for 1996–2000 (McCulloch and Midgley, 2001). They are also at odds with estimates of European and Australian emissions obtained from measurements of polluted air from these continents reaching the ALE/GAGE/AGAGE stations (Prinn *et al.*, 2001). Indeed, if these required zero-trend emissions are actually the correct ones, then the phase-out of CH_3CCl_3 consumption reported by the party nations to the Montreal Protocol must seriously be in error. This topic is expected to be studied intensively in the future. The good news is that as the emissions of CH_3CCl_3 reduce to essentially zero (as they almost are in the early 2000s), the influence of these emission errors on OH determinations becomes negligible.

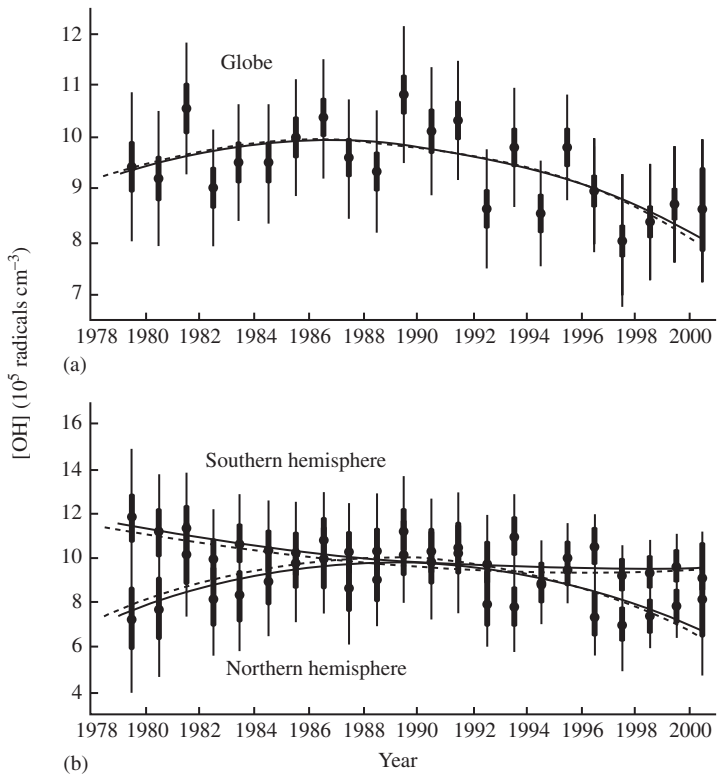

Figure 7 (a) Annual average global and (b) hemispheric OH concentrations estimated from CH_3CCl_3 measurements (after Prinn *et al.*, 2001). Uncertainties (one sigma) due to measurement errors are indicated by thick error bars and uncertainties due to both measurement, emission, and model errors are shown by thin error bars. Also shown are polynomial fits to these annual values (solid lines), and polynomials describing OH variations which were estimated directly from CH_3CCl_3 measurements (dotted lines).

Presuming that they are correct, the above positive and negative OH trends are not simply explained by the measured trends in trace gases involved in OH chemistry. There is no clear negative or positive global-scale trend in the major OH precursor gases O_3 and NO_x between 1978 and 1999, while levels of the dominant OH sink CO decreased, rather than increased, in the northern hemisphere (Prather *et al.*, 2001). At the same time, concentrations of another OH sink, CH_4, have risen significantly during 1978–1999. Prinn *et al.* (2001) have suggested that increases in tropical and subtropical countries of hydrocarbons and SO_2 that react with OH, along with a decrease of NO_x emissions in developed countries, could be involved.

Also, a growth in levels of anthropogenic aerosols could increase heterogeneous OH destruction. Such a growth in aerosols (both absorbing and reflecting) could also lower UV fluxes, through direct and indirect reflection and absorption, thus lowering OH. Neglect of these aerosol effects, as well as urban-scale chemistry, which can remove NO_x locally, may also be the reason why the higher OH levels inferred in the southern hemisphere are not simulated in many of the models in use in the early 2000s.

It is clear that further study on possible causes of OH variations of the type suggested from the CH_3CCl_3 analysis is necessary. Toward this end, the lack of long-term global-covering measurement of O_3, NO_x, SO_2, hydrocarbons, and aerosols is a very serious impediment to our understanding of OH chemistry.

4.01.7 ATMOSPHERIC MODELS AND OBSERVATIONS

A major approach for testing our knowledge of atmospheric oxidation processes has involved a careful comparison between trace gas and free radical observations and the predictions from three-dimensional (3D) CTMs that incorporate the latest understanding of homogeneous and heterogeneous fast photochemistry. While these 3D CTMs simulate qualitatively many features of the observations, there are discrepancies that point out the need for additional research. Some illustrative examples are briefly discussed here.

Berntsen *et al.* (2000) noted that their 3D CTMs indicate increases in upper tropospheric O_3 in the 1980s, whereas observations show a leveling off or a decrease. They point to the possible role of unmodeled stratospheric O_3 changes which might explain this discrepancy. Houweling *et al.* (2000) compared their 3D CTM simulations of CH_4 and CH_3CCl_3 observations providing a test of their CH_4 emission assumptions and OH concentrations. They concluded that further work is needed on simulating seasonal CH_4 emissions from wetlands and rice paddies. Spivakovsky *et al.* (2000) extensively tested their OH calculations using CH_3CCl_3, $CHClF_2$, and other trace gas data and concluded that their 3D CTM gave good agreement except in the two tropical winters (possible OH underestimates) and southern extratropics (possible OH overestimate). They noted the greater usefulness of CH_3CCl_3 for regional OH tests, as its emissions are becoming negligible.

Models have also been tested using paleodata as noted in Sections 4.01.2.2 and 4.01.5.1. Wang and Jacob (1998) noted their significant overestimation of O_3 levels in the 1800s and discussed the possible effects of incorrectly modeled surface deposition and troposphere–stratosphere exchange in producing this discrepancy. Mesoscale 3D models, which couple the dynamics of convection with cloud microphysics, and fast photochemistry have also been tested against observations; e.g., Wang and Prinn (2000) concluded that NO_x produced from lightning can deplete O_3 in the tropical Pacific upper troposphere as is often observed, but there were difficulties in simulating the observed high O_3 concentrations in the middle troposphere in these regions.

Underpinning these tests of our understanding are a large number of observational experiments using surface, aircraft, balloon and satellite platforms, and ranging from short-term campaigns to multidecadal measurement networks. Lelieveld *et al.* (1999) and Ehhalt (1999) have reviewed some of the relevant experiments focused on tropospheric oxidants. They noted the advances made in direct NO_x and HO_x observations for testing photochemical models. Thompson *et al.* (2003) have reviewed the gaps in tropospheric O_3 observations and have presented an important new data set for the southern hemisphere tropics that will provide new tests of chemical models.

4.01.8 CONCLUSIONS

Oxidation processes have played a major role in the evolution of Earth's atmosphere. Observations of trace gases and free radicals in the atmosphere in 1978–2003, and of chemicals in ice cores recording the composition of past atmospheres, are providing fundamental information about these processes. Also, basic laboratory studies of chemical kinetics, while not reviewed here, have played an essential role in defining mechanisms and rates. Models have been developed for fast photochemistry and for coupled chemical and transport processes that encapsulate current laboratory and theoretical understanding and help explain some of these atmospheric observations.

But there are important discrepancies between models and observations for OH and O_3 (both locally and globally) that still need to be resolved.

Looking into the twenty-first century, it is clear that there is urgent need to gain more observations to improve our understanding. We need much more extensive global 3D distributions for many trace gas species (O_3, CO, NO_x, reactive hydrocarbons, H_2O_2, etc.) and many more measurements of key reactive free radicals (OH, HO_2, etc.) to improve and ultimately validate models of the atmosphere. More attention needs to be given, in both modeling and observational programs, to the role of aerosols and clouds in governing UV fluxes and heterogeneous chemical reactions. Refinement of existing methods for determining long-term trends in OH, along with development of new independent approaches is clearly important.

Innovative methods for discerning the composition of past atmospheres are needed, since such information both tests current understanding and helps elucidate the process of atmospheric evolution. Finally, human and natural biospheric activities serve as the primary sources of both oxidant precursors and oxidant sink molecules, and the past, present, and possible future trends in these sources need to be much better quantified if we are to fully understand the oxidation processes in our atmosphere.

REFERENCES

Anklin M. and Bales R. C. (1997) Recent increases in H_2O_2 concentrations at Summit, Greenland. *J. Geophys. Res.* **102**, 19099–19104.

Berntsen T. K., Myhre G., Stordal F., and Isaksen I. S. A. (2000) Time evolution of tropospheric ozone and its radiative forcing. *J. Geophys. Res.* **105**, 8915–8930.

Brandenburger U., Brauers T., Dorn H.-P., Hausmann M., and Ehhalt D. H. (1998) *In-situ* measurement of tropospheric hydroxyl radicals by folded long-path laser absorption during the field campaign POPCORN in 1994. *J. Atmos. Chem.* **31**, 181–204.

Brasseur G. P., Orlando J. J., and Tyndall G. S. (1999) *Atmospheric Chemistry and Global Change*. Oxford University Press, Oxford.

Brune W. H., Stevens P. S., and Mather J. H. (1995) Measuring OH and HO_2 in the troposphere by laser-induced fluorescence at low pressure. *J. Atmos. Sci.* **52**, 3328–3336.

Chameides W. L. and Walker J. C. G. (1973) A photochemical theory of tropospheric ozone. *J. Geophys. Res.* **78**, 8751–8760.

Chameides W. L. and Walker J. C. G. (1981) Rates of fixation by lightning of carbon and nitrogen in possible primitive atmospheres. *Origins of Life* **11**, 291–302.

Chen X. and Mopper K. (2000) Determination of tropospheric hydroxyl radical by liquidphase scrubbing and HPLC: preliminary results. *J. Atmos. Chem.* **36**, 81–105.

Crosley D. R. (1995) The measurement of OH and HO_2 in the atmosphere. *J. Atmos. Sci.* **52**, 3299–3314.

Crutzen P. J. (1979) The role of NO and NO_2 in the chemistry of the troposphere and stratosphere. *Ann. Rev. Earth Planet. Sci.* **7**, 443–472.

Crutzen P. J. and Zimmerman P. H. (1991) The changing photochemistry of the trophosphere. *Tellus* **43AB**, 136–151.

Dorn H.-P., Brandenburger U., Brauers T., and Hausmann M. (1995) A new *in situ* long-path absorption instrument for the measurement of tropospheric OH radicals. *J. Atmos. Sci.* **52**, 3373–3380.

Ehhalt D. H. (1999) Gas phase chemistry of the troposphere. In *Global Aspects of Atmospheric Chemistry*, Topics in Physical Chemistry (ed. R. Zellner). Springer, Darmstadt, vol. 6, pp. 21–109.

Ehhalt D. H., Dorn H., and Poppe D. (1991) The chemistry of the hydroxyl radical in the troposphere. *Proc. Roy. Soc. Edinburgh* **97**, 17–34.

Eisele F. L. and Tanner D. J. (1991) Ion-assisted tropospheric OH measurements. *J. Geophys. Res.* **96**, 9295–9308.

Eisele F. L., Tanner D. H., Cantrell C. A., and Calvert J. G. (1996) Measurements and steady state calculations of OH concentrations at Mauna Loa Observatory. *J. Geophys. Res.* **101**, 14665–14679.

Fegley B., Prinn R. G., Hartman H., and Watkins G. H. (1986) Chemical effects of large impacts on the Earth's primitive atmosphere. *Nature* **319**, 305–308.

Felton C. C., Sheppard J. C., and Campbell M. J. (1990) The radiochemical hydroxyl radical measurement method. *Environ. Sci. Technol.* **24**, 1841–1847.

Folland C. K., Karl T. R., Christy J. R., Clarke R. A., Gruza G. V., Jouzel J., Mann M. E., Oerlemans J., Salinger M. J., and Wang S. W. (2001) Observed climate variability and change. In *Climate Change 2001: The Scientific Basis* (ed. J. T. Houghton), Cambridge University Press, New York, pp. 99–181.

Haan D., Martinerie P., and Raynaud D. (1996) Ice core data of atmospheric carbon monoxide over Antarctica and Greenland during the last 200 years. *Geophys. Res. Lett.* **23**, 2235–2238.

Hard T. M., O'Brien R. J., Chan C. Y., and Mehrabzadeh A. A. (1984) Tropospheric free radical determination by FAGE. *Environ. Sci. Technol.* **18**, 768–777.

Hard T. M., George L. A., and O'Brien R. J. (1995) FAGE Determination of Tropospheric HO and HO_2. *J. Atmos. Sci.* **52**, 3354–3372.

Hofzumahaus A., Aschmutat U., Hebling M., Holland F., and Ehhalt D. (1996) The measurement of tropospheric OH radicals by laser-induced fluorescence spectroscopy during the POPCORN field campaign. *Geophys. Res. Lett.* **23**, 2541–2544.

Holland F., Hessling M., and Hofzumahaus A. (1995) *In-situ* measurement of tropospheric OH radicals by laser-induced fluorescence. A description of the KFA instrument. *J. Atmos. Sci.* **52**, 3393–3401.

Holland H. D. (1984) *The Chemical Evolution of the Atmosphere and Oceans*. Princeton University Press, Princeton.

Hough A. M. and Derwent R. G. (1990) Changes in the global concentration of tropospheric ozone due to human activities. *Nature* **344**, 645–648.

Houweling S., Dentener F., and Lelieveld J. (2000) The modeling of tropospheric methane: how well can point measurements be reproduced by a global model? *J. Geophys. Res.* **105**, 8981–9002.

Huang J. and Prinn R. (2002) Critical evaluation of emissions for potential gases for OH estimation. *J. Geophys. Res.* **107**, D24, 4784, doi: 10.1029/2002 JD002394.

Krol M., van Leeuwen P. J., and Leileveld J. (1998) Global OH trend inferred from methyl chloroform measurements. *J. Geophys. Res.* **103**, 10697–10711.

Krol M., van Leeuwen P. J., and Lelieveld J. (2001) Reply to comment by Prinn and Huang (2001) on Krol *et al*. (1998) *J. Geophys. Res.* **106**, 23158–23168.

Lange M. A. and Ahrens T. J. (1982) The evolution of an impact-generated atmosphere. *Icarus* **51**, 96–120.

Lelieveld J., Thompson A. M., Diab R. D., Hov O., Kley D., Logan J. A., Nielson O. J., Stockwell W. R., and Zhou X. (1999) Tropospheric ozone and related processes.

In *Scientific Assessment of Ozone Depletion: 1998* (ed. D. Albritton). World Meteorological Organization, Geneva, pp. 8.1–8.42.

Levine J. S. (1985) The photochemistry of the early atmosphere. In *The Photochemistry of Atmospheres* (ed. J. S. Levine). Academic Press, Orlando, pp. 3–38.

Levy H. (1971) Normal atmosphere: large radical and formaldehyde concentrations predicted. *Science* **173**, 141–143.

Levy H., Kasibhatla P. S., Moxim W. J., Klonecki A., Hirsch A., Oltmans S., and Chameides W. L. (1997) The global impact of human activity on tropospheric ozone. *Geophys. Res. Lett.* **24**, 791–794.

Lewis J. and Prinn R. (1984) *Planets and their Atmospheres: Origin and Evolution*. Academic Press, Orlando.

Logan J., Prather M., Wofsy S., and McElroy M. (1981) Tropospheric chemistry: a global perspective. *J. Geophys. Res.* **86**, 7210–7254.

Madronich S. and Granier C. (1992) Impact of recent total ozone changes on tropospheric ozone photodissociation, hydroxyl radicals, and methane trends. *Geophys. Res. Lett.* **19**, 465–467.

Mak J. E., Brenninkmeijer C. A. M., and Tamaresis J. (1994) Atmospheric ^{14}CO observations and their use for estimating carbon monoxide removal rates. *J. Geophys. Res.* **99**, 22915–22922.

Marenco A., Gouget H., Nedelec P., and Pages J. P. (1994) Evidence of long-term increase in tropospheric ozone from Pic du Midi data series, consequences and positive radiative forcing. *J. Geophys. Res.* **99**, 16617–16632.

McCulloch A. and Midgley P. (2001) The history of methyl chloroform emissions: 1951–2000. *Atmos. Environ.* **35**, 5311–5319.

Miller B. R., Weiss R. F., Prinn R. G., Huang J., and Fraser P. J. (1998) Atmospheric trend and lifetime of chlorodifluoromethane (HCFC-22) and the global tropospheric OH concentration. *J. Geophys. Res.* **103**, 13237–13248.

Montzka S. A., Spivakovsky C. M., Butler J. H., Elkins J. W., Lock L. T., and Mondecl D. J. (2000) New observational constraints on atmospheric hydroxyl on global and hemispheric scales. *Science* **288**, 500–503.

Mount G. H. (1992) The measurement of tropospheric OH by long-path absorption: 1. Instrumentation. *J. Geophys. Res.* **97**, 2427–2444.

Mount G. H. and Harder J. W. (1995) The measurement of tropospheric trace gases at Fritz Peak Observatory by long-path absorption: OH and ancillary gases. *J. Atmos. Sci.* **52**, 3342–3353.

Penner J., Andreae M., Annegarn H., Barrie L., Feichter J., Hegg D., Jayaraman A., Leaitch R., Murphy D., Nganga J., and Pitari G. (2001) Aerosols: their direct and indirect effects. In *Climate Change 2001: The Scientific Basis* (ed. J. T. Houghton). Cambridge University Press, New York, pp. 289–348.

Poppe D., Zimmerman J., Bauer R., Brauers T., Bruning D., Callies J., Dorn H. P., Hofzumahaus A., Johnen F. J., Khedim A., Koch H., Koppman R., London H., Muller K. P., Neuroth R., Plass-Dulmer C., Platt U., Rohrer F., Roth E. P., Rudolph J., Schmidt U., Wallasch M., and Ehhalt D. H. (1994) Comparison of measured OH concentrations with model calculations. *J. Geophys. Res.* **99**, 16633–16642.

Poppe D., Zimmerman J., and Dorn H. P. (1995) Field data and model calculations for the hydroxyl radical. *J. Atmos. Sci.* **52**, 3402–3407.

Prather M., Ehhalt D., Dentener F., Derwent R., Dlugokencky E., Holland E., Isaksen I., Katima J., Kirchhoff V., Matson P., Midgley P., and Wang M. (2001) Atmospheric chemistry and greenhouse gases. In *Climate Change 2001: The Scientific Basis* (ed. J. T. Houghton). Cambridge University Press, New York, pp. 239–288.

Prinn R. (1982) Origin and evolution of planetary atmospheres: an introduction to the problem. *Planet. Space Sci.* **30**, 741–753.

Prinn R. (1994) The interactive atmosphere: global atmospheric–biospheric chemistry. *Ambio* **23**, 50–61.

Prinn R. and Fegley B. (1987) Bolide impacts, acid rain, and biospheric traumas at the Cretaceous–Tertiary boundary. *Earth Planet. Sci. Lett.* **83**, 1–15.

Prinn R. and Huang J. (2001) Comment on Krol *et al*. (1998). *J. Geophys. Res.* **106**, 23151–23157.

Prinn R., Rasmussen R., Simmonds P., Alyea F., Cunnold D., Lane B., Cardelino C., and Crawford A. (1983) The atmospheric lifetime experiment 5. Results for CH_3CCl_3 based on three years of data. *J. Geophys. Res.* **88**, 8415–8426.

Prinn R., Cunnold D., Simmonds P., Alyea F., Boldi R., Crawford A., Fraser P., Gutzler D., Hartley D., Rosen R., and Rasmussen R. (1992) Global average concentration and trend for hydroxyl radicals deduced from ALE/GAGE trichloroethane (methyl chloroform) data for 1978–1990. *J. Geophys. Res.* **97**, 2445–2461.

Prinn R., Jacoby H., Sokolov A., Wang C., Xiao X., Yang Z., Eckhaus R., Stone P., Ellerman D., Melillo J., Fitzmaurice J., Kicklighter D., Holian G., and Liu Y. (1999) Integrated global system model for climate policy assessment: feedbacks and sensitivity studies. *Climat. Change* **41**, 469–546.

Prinn R., Weiss R., Fraser P., Simmonds P., Cunnold D., Alyea F., O'Doherty S., Salameh P., Miller B., Huang J., Wang R., Hartley D., Harth C., Steele L., Sturrock G., Midgley P., and McColloch A. (2000) A history of chemically and radiatively important gases in air deduced from ALE/GAGE/AGAGE. *J. Geophys. Res.* **105**, 17751–17792.

Prinn R. G. (2000) Measurement equation for trace chemicals in fluids and solution of its inverse. In *Inverse Methods in Global Biogeochemical Cycles Geophysical Monograph* (ed. P. Kasibhatla). American Geophysical Union, Washington, DC, vol. 114, pp. 3–18.

Prinn R. G., Cunnold D. M., Rasmussen R., Simmonds P. G., Alyea F. N., Crawford A., Fraser P. J., and Rosen R. (1987) Atmospheric trends in methylchloroform and the global average for the hydroxyl radical. *Science* **238**, 945–950.

Prinn R. G., Weiss R. F., Miller B. R., Huang J., Alyea F. N., Cunnold D. M., Fraser P. J., Hartley D. E., and Simmonds P. G. (1995) Atmospheric trends and lifetime of CH_3CCL_3 and global OH concentrations. *Science* **269**, 187–192.

Prinn R. G., Huang J., Weiss R. F., Cunnold D. M., Fraser P. J., Simmonds P. G., McCulloch A., Harth C., Salameh P., O'Doherty S., Wang R. H. J., Porter L., and Miller B. R. (2001) Evidence for substantial variations of atmospheric hydroxyl radicals in the past two decades. *Science* **292**, 1882–1888.

Quay P., King S., White D., Brockington M., Plotkin B., Gammon R., Gerst S., and Stutsman J. (2000) Atmospheric ^{14}CO: a tracer of OH concentration and mixing rates. *J. Geophys. Res.* **105**, 15147–15166.

Sigg A. and Neftel A. (1991) Evidence for a 50% increase in H_2O_2 over the past 200 years from a Greenland ice core. *Nature* **351**, 557–559.

Simmonds P. G., O'Doherty S., Huang J., Prinn R., Derwent R., Ryall D., Nickless G., and Cunnold D. (1998) Calculated trends and the atmospheric abundance of 1,1,1,2-tetrafluoroethane, 1,1-dichloro-1-fluoroethane, and 1-chloro-1, 1-difluorethane using automated *in situ* gas chromatography-mass spectrometry measurements recorded at Mace Head, Ireland, from October 1994 to March 1997. *J. Geophys. Res.* **103**, 16029–16037.

Spivakovsky C. M., Logan J. A., Montzka S. A., Balkanski Y. J., Foreman-Fowler M., Jones D. B. A., Horowitz L. W., Fusco A. C., Brenninkmeijer C. A. M., Prather M. J., Wofsy S. C., and McElroy M. B. (2000) Three dimensional climatological distribution of tropospheric OH: update and evaluation. *J. Geophys. Res.* **105**, 8931–8980.

Staffelbach T. A., Neftel A., Stauffer B., and Jacob D. J. (1991) Formaldehyde in polar ice cores: a possibility to characterize the atmospheric sink of methane in the past? *Nature* **349**, 603–605.

Stimpfle R. M. and Anderson J. G. (1988) *In situ* detection of OH in the lower stratosphere with a balloon borne high repetition rate laser system. *Geophys. Res. Lett.* **15**, 1503–1506.

Tanner D. J., Jefferson A., and Eisele F. L. (1997) Selected ion chemical ionization mass spectrometric measurement of OH. *J. Geophys. Res.* **102**, 6415–6425.

Thompson A. M. (1992) The oxidizing capacity of the Earth's atmosphere: probable past and future changes. *Science* **256**, 1157–1165.

Thompson A. M., Witte J. C., Mc Peters R. D., Oltmans S. J., Schmidlin F. J., Logan J. A., Fujiwara M., Kirchoff V., Posny F., Coetzee G., Hoegger B., Kawakami S., Ogawa T., Johnson B., Vomel H., and Labow G. (2003) The 1998–2000 SHADOZ Tropical Ozone Climatology: comparison with TOMS and ground-based measurements. *J. Geophys. Rev.* **108**, D2, 8238, doi: 10.1029/2001 JD000967.

Volz A. and Kley D. (1988) Evaluation of the Montsouris Series of ozone measurements made in the nineteenth century. *Nature* **332**, 240–242.

Volz A., Ehhalt D. H., and Derwent R. G. (1981) Seasonal and latitudinal variation of ^{14}CO and the tropospheric concentration of OH radicals. *J. Geophys. Res.* **86**, 5163–5171.

Wang C. and Prinn R. G. (1999) Impact of emissions, chemistry and climate on atmospheric carbon monoxide: 100-year predictions from a global chemistry model. *Chemosph. Global Change* **1**, 73–81.

Wang C. and Prinn R. G. (2000) On the roles of deep convective clouds in tropospheric chemistry. *J. Geophys. Res.* **105**, 22269–22297.

Wang Y. and Jacob D. J. (1998) Anthropogenic forcing on tropospheric ozone and OH since pre-industrial times. *J. Geophys. Res.* **103**, 31123–31135.

Treatise On Geochemistry
ISBN (set): 0-08-043751-6
Volume 4; (ISBN: 0-08-044339-7); pp. 1–19